

The Effect of Datum Constraints for Terrestrial Laser Scanner Self-Calibration

**Mohd Azwan ABBAS, Halim SETAN, Zulkepli MAJID, Khairulnizam M. IDRIS and
Mohd Farid MOHD ARIFF, Malaysia
Albert K. CHONG, Australia
Derek D. LICHTI, Canada**

Key words: Terrestrial laser scanner, self-calibration, network configuration, datum constraints.

SUMMARY

Similar to other optical and electronic instruments, data obtained from terrestrial laser scanners (TLS) can be impaired with errors coming from different sources. Thus, a calibration routine is crucial to ensure the quality of the TLS data. Self-calibration is a common camera calibration procedure used for photogrammetric measurement that has been adapted for TLS application. According to the photogrammetric approach, there are several network configuration and datum constraints conditions that needed to be fulfilled in the calibration process. However, network configurations applied to TLS self-calibration are quite different compared to photogrammetry. Regarding the datum constraints, the theory states that the selection of either inner or minimum constraints can cause different effects on parameter correlations. Due to this argument, this study investigates the possible effect of datum constraints selection in TLS self-calibration. Three comparisons were carried out between the results obtained from inner and minimum datum constraints. By applying graphical and statistical approaches, the differences were analysed and the results indicated that both datum constraints offer similar outcomes and parameter correlations.

The Effect of Datum Constraints for Terrestrial Laser Scanners Self-Calibration

Mohd Azwan ABBAS, Halim SETAN, Zulkepli MAJID, Khairulnizam M. IDRIS and Mohd Farid MOHD ARIFF, Malaysia
Albert K. CHONG, Australia
Derek D. LICHTI, Canada

1. INTRODUCTION

Terrestrial laser scanners (TLS) are active sensors which are capable of directly capturing three dimensional (3D) spatial data (point clouds). With the rapid increase in capture speed and measurement accuracy, the dense point clouds acquired by TLS makes the task of producing 3D models much easier. The current TLS has considerably improved the capture procedure and the quality of final product in 3D modelling. Compared with other 3D capture approaches, the task of processing that involves constructing complete 3D models using TLS software becomes easier and faster. Furthermore, current TLS can also capture images using either an attached or a built-in camera. This integration (i.e. TLS and camera) allows current TLS also has the capability to provide colourized point clouds which allow the production of photorealistic 3D models.

Although, TLS is able to provide high resolution point clouds, that's only can guarantee the measurement precision. There are some applications requiring accurate spatial information such as reverse engineering, industrial measurement and deformation monitoring. According to Abdul and Halim (2001), there is a difference between precision and accuracy. Precision is defined as the closeness of the agreement between independent test results compared to the mean value. Accuracy is defined as the closeness of the agreement between the result of a measurement and its true value. That means, even if a scanner is able to give better precision, it is not necessarily able to provide more accurate information. In order to capture accurate data, TLS measurement accuracy must be investigated, and these instruments must be calibrated relating to instrumental and non-instrumental errors.

There are two calibration approaches available: 1) component, and 2) system calibration. Due to the requirement of special laboratories and tools to perform component calibration, it cannot be implemented by most TLS users (Azwan et al., 2013). In contrast, system calibration only requires a room with appropriate targets as applied for this study.

Since the TLS self-calibration was adapted from photogrammetry, thus the datum constraints applied for TLS self-calibration are also similar to photogrammetry self-calibration. There are generally two types of constraints applied: 1) minimum; and 2) inner constraints. However, according to Reshetyuk (2009), both datum constraints (used in photogrammetry calibration)

have their own limitations. The use of minimum constraints tends to cause large correlations between object points and some of the calibration parameters. The inner constraints have the unfavourable property of increasing the correlations between the calibration parameters and the exterior orientation parameters. Reshetyuk (2009) has raised similar issue for TLS calibration. The author developed a unified approach using bundle adjustment in order to reduce the correlations between the parameters.

However, most of the TLS calibration researchers were using parametric equation to perform bundle adjustment either using minimum (Gieldorf et al., 2004; Mohd Azwan et al., 2013) or inner constraints (Lichti, 2007; Schneider, 2009; Lichti and Chow, 2013). Even though self-calibration was adapted from photogrammetry, the requirements for the network configuration (e.g. target distribution, calibration field and positions of the sensor) for the self-calibration for TLS (Lichti, 2007) and photogrammetry (Fraser, 1996) are quite different. With the intention to investigate this issue, this study performed a self-calibration for Faro Focus 3D scanner. Both datum constraints were imposed on the bundle adjustment and the results were statistically analysed to determine whether there is any significant difference in correlation between the calculated parameters.

2. GEOMETRIC MODEL FOR SELF-CALIBRATION

Due to the very limited knowledge regarding the inner functioning of modern terrestrial laser scanners, most researchers have introduced assumptions about a suitable error model for TLS based on errors found in reflectorless total stations (Lichti, 2007). Since the data measured by TLS are range, horizontal and vertical angle, the equations for each measurement are augmented with systematic error correction model as follows (Reshetyuk, 2009):

$$\text{Range, } r = \sqrt{x^2 + y^2 + z^2} + \Delta r \quad (1)$$

$$\text{Horizontal direction, } \varphi = \tan^{-1}\left(\frac{x}{y}\right) + \Delta\varphi \quad (2)$$

$$\text{Vertical angle, } \theta = \tan^{-1}\left(\frac{z}{\sqrt{x^2 + y^2}}\right) + \Delta\theta \quad (3)$$

Where,

x, y, z = Cartesian coordinates of point in scanner space.

$\Delta r, \Delta\varphi, \Delta\theta$ = Systematic error model for range, horizontal angle and vertical angle, respectively.

Since this study was carried out on a panoramic scanner (the Faro Focus 3D), the angular observations computed using equation (2) and equation (3) must be modified. This is due to the scanning principles applied by panoramic scanner, which rotates only through 180° to provide 360° information for horizontal and vertical angles as depicted in Fig. 1.

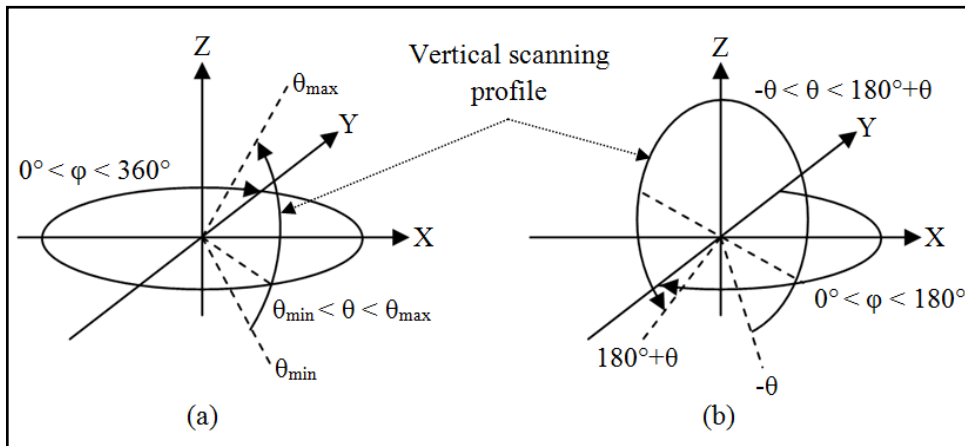


Figure 1: Angular observation ranges for (a) Hybrid scanner and (b) Panoramic scanner.

Based on Lichti (2010), the modified mathematical model for a panoramic scanner can be presented as follows:

$$\varphi = \tan^{-1}\left(\frac{x}{y}\right) - 180^\circ \quad (4)$$

$$\theta = 180^\circ - \tan^{-1}\left(\frac{z}{\sqrt{x^2 + y^2}}\right) \quad (5)$$

The modified models above (4 and 5) are only applicable when the horizontal angle is more than 180° as shown in Fig. 1. Otherwise, equation (2) and (3) will be used, which means that panoramic scanner required two equations for both angular observations.

According to Lichti (2010), the systematic error models can be classified into two groups, physical and empirical parameters. The first group can comprise the basic calibration parameters which have been derived from the total station systematic error models. This group includes the constant, cyclic, trunnion axis, collimation axis and vertical circle index errors and those as described in Lichti and Licht (2006). The other group of error models is not necessarily apparent and may be due to geometric defects in construction and/or electrical cross-talk and may be system dependent. These are inferred from systematic trends visible in the residuals of a highly-redundant and geometrically strong, minimally-constrained least-square adjustment. Lichti (2007) has identified 21 systematic errors model from phase-based scanner (Faro 880).

However, this study focuses on the most significant systematic errors model as applied by Reshetyuk (2009) in his study as follows:

i. Systematic error model for range. (6)

$$\Delta r = a_0$$

ii. Systematic error model for horizontal angle. (7)

$$\Delta \varphi = b_0 \sec \theta + b_1 \tan \theta$$

iii. Systematic error model for vertical angle. (8)

$$\Delta \theta = c_0$$

Where,

a_0 = Constant rangefinder offset error

b_0 = Collimation axis error

b_1 = Trunnion axis error

c_0 = Vertical circle index error

According to Lichti et al. (2011), systematic error models for panoramic scanner can be recognised based on the trends in the residuals of least squares adjustments that exclude the relevant calibration parameters. In most cases, the trend of un-modelled systematic error closely resembles the analytical form of the corresponding correction model.

In order to perform the self-calibration bundle adjustment, the x, y, z laser scanner coordinates have to be expressed as functions of the position and orientation of the laser scanner in a global coordinate system (Schneider, 2009). Based on rigid-body transformation, for the j^{th} target scanned from the i^{th} scanner station, the equation is as follows:

$$\begin{aligned} x &= R_{11}(X_j - X_{si}) + R_{21}(Y_j - Y_{si}) + R_{31}(Z_j - Z_{si}) \\ y &= R_{12}(X_j - X_{si}) + R_{22}(Y_j - Y_{si}) + R_{32}(Z_j - Z_{si}) \\ z &= R_{13}(X_j - X_{si}) + R_{23}(Y_j - Y_{si}) + R_{33}(Z_j - Z_{si}) \end{aligned} \quad (9)$$

Where,

$\begin{bmatrix} x & y & z \end{bmatrix}$ = Coordinates of the target in the scanner coordinate system

${}_3R_3$ = Components of rotation matrix between the two coordinate systems for the i^{th} scanner station

$\begin{bmatrix} X_j & Y_j & Z_j \end{bmatrix}$ = Coordinates of the j^{th} target in the global coordinate system

$\begin{bmatrix} X_{si} & Y_{si} & Z_{si} \end{bmatrix}$ = Coordinates of the i^{th} scanner station in the global coordinate system

3. Datum Constraints

Three-dimensional photogrammetric networks generally require seven datum constraints to remove datum defects. With the range observation implicitly defining the network scale, and this means that a TLS network only requires six datum constraints.

According to Reshetyuk (2009), a minimum of six fixed coordinates distributed over 3 non-collinear points is required in order to implement minimum constraints. Based on the camera calibration approach, Fraser (1984) mentioned that an optimum choice of the points to fix is that the centroid of these points is reasonably close to the centre of the target array, and the area of the triangle they define is maximal. In order to use the minimum constraints, this study has fixed the exterior orientation parameters for the first scanner station. Based on the original shape of design matrix A as shown in equation (10) and (11), the process of removing matrix element for minimum constraints can be expressed as follows:

$$\begin{aligned}
 {}_n A_u &= [A_{EO} \quad A_{CP} \quad A_{TG}] \\
 &= \begin{bmatrix} A_{EO_1} & 0 & 0 & A_{CP} & A_{TG} \\ 0 & A_{EO_2} & 0 & A_{CP} & A_{TG} \\ 0 & 0 & A_{EO_n} & A_{CP} & A_{TG} \end{bmatrix} \quad (10)
 \end{aligned}$$

Removed

Where,

n = number of observations

u = number of unknown parameters

A_{EO} = design matrix for exterior orientation (EO) parameters

A_{CP} = design matrix for calibration parameters (CP)

A_{TG} = design matrix for object points (TG)

New design matrix A without EO parameters for first scanner station is in the form:

$${}_n A_u = \begin{bmatrix} 0 & 0 & A_{CP} & A_{TG} \\ A_{EO_2} & 0 & A_{CP} & A_{TG} \\ 0 & A_{EO_n} & A_{CP} & A_{TG} \end{bmatrix} \quad (11)$$

Application of the inner constraints for this study has been adopted from Lichti (2007). The constraint imposed on object points (TG) to remove the datum defects are given in matrix form as:

$$[0 \quad 0 \quad G_o^T] \begin{bmatrix} \hat{X}_{EO} \\ \hat{X}_{CP} \\ \hat{X}_{TG} \end{bmatrix} = [0] \quad (12)$$

Where,

\hat{X}_{EO} = Vector of the exterior orientation parameters

\hat{X}_{CP} = Vector of the calibration parameters

\hat{X}_{TG} = Vector of the object points

The true form of the datum design constraint matrix G_o is as follows (Kuang, 1996).

$$G_o^T = \left(\begin{array}{ccc|ccc|ccc} 1 & 0 & 0 & 1 & 0 & 0 & 1 & 0 & 0 \\ 0 & 1 & 0 & 0 & 1 & 0 & 0 & 1 & 0 \\ 0 & 0 & 1 & 0 & 0 & 1 & 0 & 0 & 1 \\ 0 & Z_1 & -Y_1 & 0 & Z_2 & -Y_2 & 0 & Z_n & -Y_n \\ -Z_1 & 0 & X_1 & -Z_2 & 0 & X_2 & -Z_n & 0 & X_n \\ Y_1 & -X_1 & 0 & Y_2 & -X_2 & 0 & Y_n & -X_n & 0 \end{array} \right) \quad (13)$$

The bordered system of normal equation follows from the standard parametric least square is given as:

$$N \hat{X} + U = 0$$

$$\begin{bmatrix} A^T P A & G_o^T \\ G_o & 0 \end{bmatrix} \begin{bmatrix} \hat{X}_{EO} \\ \hat{X}_{CP} \\ \hat{X}_{TG} \\ k_c \end{bmatrix} + \begin{bmatrix} A^T P L \\ 0 \end{bmatrix} = \begin{bmatrix} 0 \\ 0 \end{bmatrix} \quad (14)$$

Where,

A = Design matrix

P = Weight matrix

L = Observations matrix

k_c = Vector of Lagrange multipliers

4. EXPERIMENT

As shown in Fig. 2, a self-calibration target field was established in a laboratory with dimensions 9m x 7m x 2.6m. The 123 planar targets were distributed on the four walls and ceiling based on conditions stated by Lichti (2007).

Seven scan stations were used to observe the targets. As shown in Fig. 3, four scan stations were located at the corners and one at the centre of the room. The other two were positioned close to the two corners with the scanner orientation manually rotated 90° from scanner orientation at the same corner. In all cases, the height of the scanner was midway between the floor and the ceiling.



Figure 2: Self-calibration test field for the Faro Focus 3D scanner.

In this experiment, the scan resolution was set to the 1/4 setting which is equivalent to the medium resolution. Higher resolution scans were not captured due to the longer time required to complete the scanning. Furthermore, medium resolution was sufficient for Faroscene software to extract all targets except those which have high incidence angles (e.g. 70° and above).

After the scanning and target measurement processes were completed, the bundle adjustment was performed. The precision settings used to compute the observation weights were based on the manufacturer's specifications (i.e. 2mm for distance and 0.009° for both angle measurements). After 4 iterations, both (inner and minimum constraints) bundle adjustment process converged successfully.

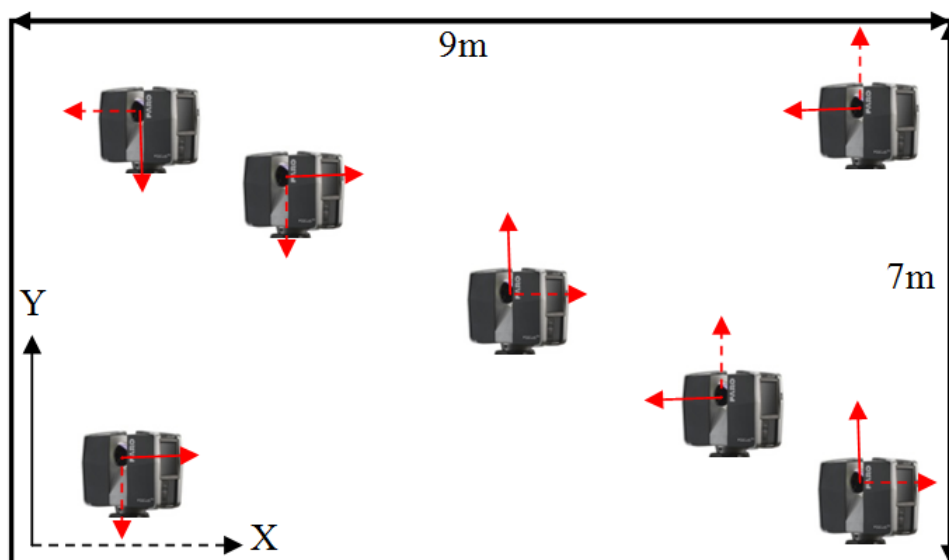


Figure 3: Scanner locations during self-calibration.

There are three sets of parameters produced by the self-calibration bundle adjustments:

- i. The exterior orientation parameters which consist of 3 translations and 3 rotations.
- ii. The calibration parameters for range, horizontal and vertical angles.
- iii. The adjusted coordinates of the targets or also known as object points in photogrammetry.

To evaluate the effect of datum constraints selection, correlation coefficient values are extracted from variance-covariance matrix using the following formula (Abdul and Halim, 2001):

$$\rho_{x_i x_j} = \frac{\sigma_{x_i x_j}}{\sigma_{x_i} \sigma_{x_j}} \quad (15)$$

Where,

$\sigma_{x_i x_j}$ = Element of variance covariance matrix.

σ_{x_i} = Standard deviation of the parameter.

The extracted correlation coefficients were grouped into two categories: 1) calibration parameters and exterior orientations, and 2) calibration parameters and object points. For assessment purposes, several graphs were plotted to visualise the different between the parameter correlations of inner and minimum constraints. Statistical analysis was carried out to evaluate the results obtained from the plotted graphs. In this study, the one-way between groups ANOVA was used to analyse the variation between the populations mean for the groups. The F-variance ratio test was used to investigate the significance of the difference between two populations (Gopal, 1999). The population's variance belongs to parameter correlations yielded from bundle adjustment using inner and minimum constraints. The hypothesis of the test is:

H_0 : The two population variances are not significantly different from each other.

H_A : The two population variances are significantly different from each other.

The F-Test was carried out using the formula:

$$F = \frac{\sigma_1^2}{\sigma_2^2} \quad (16)$$

Where,

σ_1^2 = Variance of population 1.

The null hypothesis (H_0) is rejected if the calculated F value (Eq. 16) is higher than the critical F value (predicted from the F-distribution table) at the 5% significance level. The rejection of H_0 shows that the test parameters are not equal. If the test shows no significant difference, then both datum constraints are suitable for the self-calibration bundle adjustment for terrestrial laser scanner.

5. RESULTS AND ANALYSIS

The estimated calibration parameters given in equations (6)-(8) for the adjustments using both datum constraints are shown in Table I.

Table 1: Calibration parameters and their standard deviations

Calibration parameters	Inner constraints	Minimum constraints
Constant range error, a_0	$-1.3\text{mm} \pm 0.9\text{mm}$	$-1.3\text{mm} \pm 0.9\text{mm}$
Collimation axis error, b_0	$-14.3'' \pm 2.5''$	$-14.3'' \pm 2.5''$
Trunnion axis error, b_1	$-35.2'' \pm 7.5''$	$-35.2'' \pm 7.5''$
Vertical circle index error, c_0	$-24.1'' \pm 3.2''$	$-24.1'' \pm 3.2''$

As can be seen in Table 1, all calculated parameters are the same, which is expected since the interior parameters are invariant with respect to minimum datum definition. As a prior assumption, hypothesis can be made that there are no significant effect in datum constraints selection for TLS self-calibration bundle adjustment.

To investigate the impact of datum constraints selection on parameter correlations in self-calibration, Figs. 4 - 8 show the correlations between calibration parameters, exterior orientation and object points.

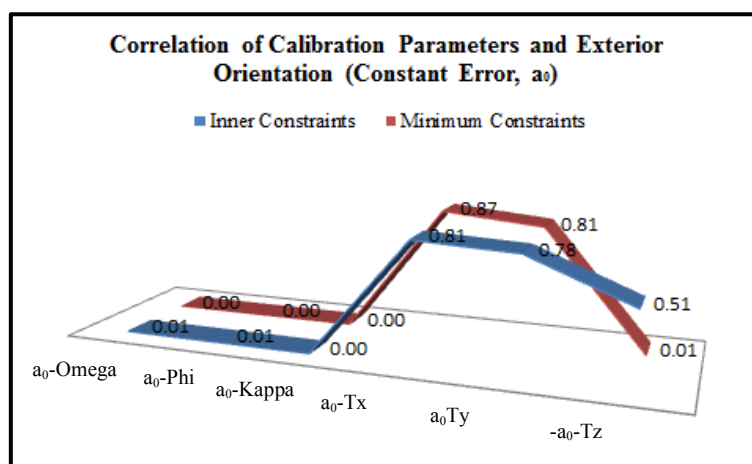


Figure 4: Parameter correlations of the constant range error (a_0) and the exterior orientation parameters.

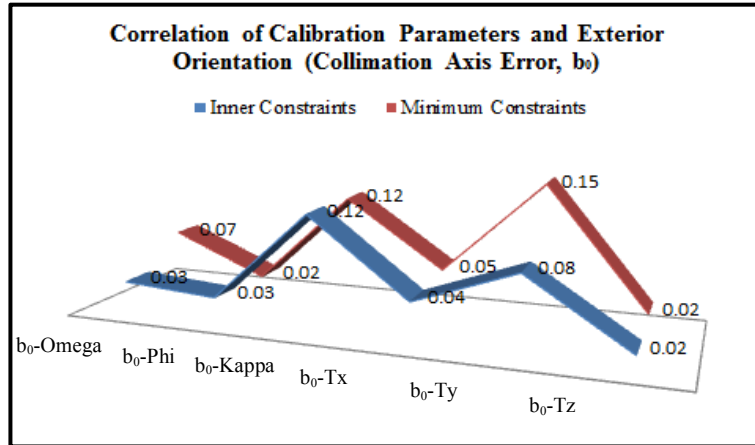


Figure 5: Parameter correlations of the collimation axis error (b_0) and the exterior orientation parameters.

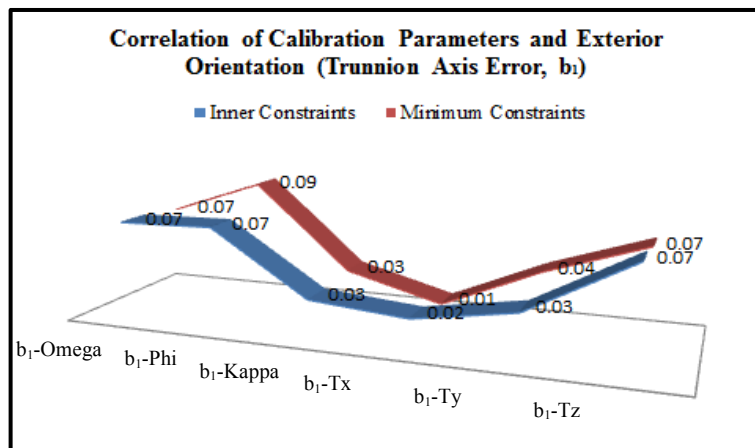


Figure 6: Parameter correlations of the trunnion axis error (b_1) and the exterior orientation parameters.

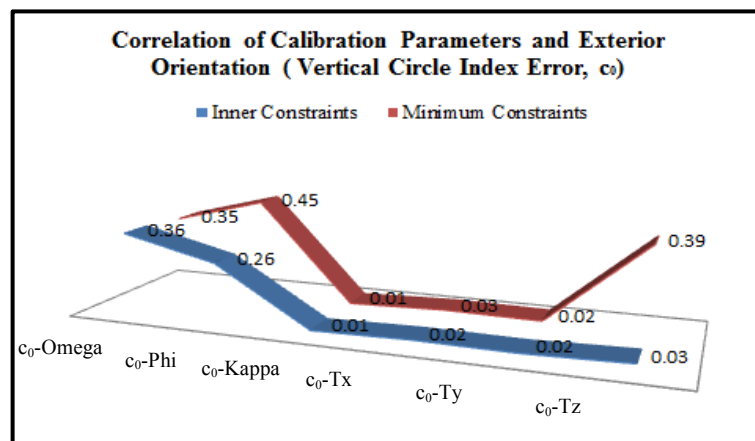


Figure 7: Parameter correlations of the vertical circle index error (c_0) and the exterior orientation parameters.

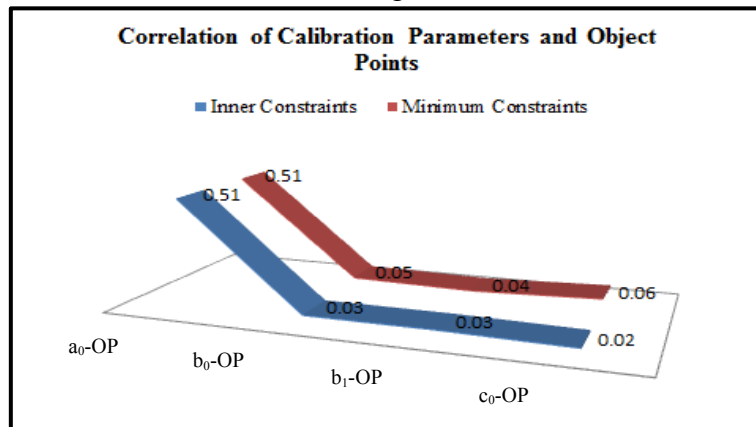


Figure 8: Parameter correlations of all four calibration parameters (a_0 , b_0 , b_1 and c_0) and the object points.

As discussed in Section 1, the selection of datum constraints in photogrammetry self-calibration can have different effects on the parameter correlations. The use of inner constraints increased the correlations between the calibration parameters and the exterior orientation parameters. However, employing minimum constraints tends to cause large correlations between object points and calibration parameters. According what is known from close-range photogrammetry self-calibration, the results of the inner constraints (blue colour in Figs. 4-7) should be larger compared to the minimum constraints (red colour). The results obtained for TLS self-calibration are quite similar. The parameter correlations yielded from both datum constraints are balanced. In certain cases, inner constraints have caused larger correlations as shown in Fig. 4, which have maximum different, 0.5. However, the minimum constraints as well have exemplified in Fig. 5 to Fig. 7 that the method results in larger correlations compared to inner constraints, 0.07, 0.36 and 0.02, respectively. A similar situation is illustrated in Fig. 8 that shows that the maximum correlation difference between datum constraints is only 0.04, which is insignificant. In other words, through graphical evaluation, the initial conclusion can be made that the selection of datum constraints does not significantly affect the parameter correlations.

To obtain a concrete conclusion, statistical analyses have been employed to demonstrate that the impacts of datum constraints selection found in close-range photogrammetry aren't necessarily applicable in TLS self-calibration. In this analysis, the ANOVA test was used to statistically verify that the selection of datum constraints for TLS self-calibration bundle adjustment does not affect the parameter correlations. The results of the F-variance ratio test with 95% confidence level show that the difference between the means for all tables were not significant. In all cases, the calculated F values are smaller than critical F (Table II) and p-values computed from the test are larger than the level of significance (0.05). Thus, the null hypothesis (H_0) was accepted. With acceptance of the null hypothesis, a conclusion can be made that both datum constraints contribute similar parameter correlations. In other words,

the selection of inner or minimum datum constraint does not affect the calculated calibration parameters and the parameter correlations.

Table II: Result of ANOVA test.

Tested Parameters	Calculated F	>/<	Critical F	p-value	>/<	Level of Significance
a_0 – Exterior Orientations	0.09	<	5.05	0.77	>	0.05
b_0 – Exterior Orientations	0.42	<	5.05	0.53	>	0.05
b_1 – Exterior Orientations	0.01	<	5.05	0.91	>	0.05
c_0 – Exterior Orientations	0.69	<	5.05	0.42	>	0.05
a_0, b_0, b_1, c_0 – Object points	0.01	<	9.28	0.92	>	0.05

6. CONCLUSION

A self-calibration procedure used to estimate systematic errors in TLS is a method adapted from the photogrammetric approach. There are several considerations need be accounted for in order to perform this calibration method, especially the network design and the choice of datum definition. In close-range photogrammetry it is known that the selection of datum constraints can affect the parameter correlations. However, self-calibration for TLS has different requirements for the network configuration compared. Therefore, this study carried out several experiments to investigate the effect of datum constraints selection for TLS self-calibration. The results verify that both inner and minimum datum constraints result in similar parameter correlations, which mean that the datum-dependence problem in photogrammetry does not directly apply to TLS self-calibration.

REFERENCES

- Abdul, W. I. and Halim, S. (2001). *Pelajaran Ukur*. Kuala Lumpur: Dewan Bahasa dan Pustaka, 2001:5-9.
- Fraser, C. S. (1984). Network Design Considerations for Non-Topographic Photogrammetry. *Photogrammetric Engineering and Remote Sensing*, 50(8), 1984: 1115-1126.
- Fraser, C. S. (1996) *Network Design*. In *Close Photogrammetry and Machine Vision*. Edited by K. B. Atkinson. Whittles Publishing, Roseleigh House, Latheronwheel, Scotland, UK, 1996:256-279.
- Gielsdorf, F., Rietdorf, A. and Gruendig, L. (2004). A Concept for the Calibration of Terrestrial Laser Scanners. *TS26 Positioning and Measurement Technologies and Practices II-Laser Scanning and Photogrammetry*. FIG Working Week 2004, Athens, Greece: 1-10.
- Gopal, K. K. (1999). 100 Statistical Test. Thousand Oaks, California: SAGE Publications Ltd., 1999:37-38.

Gopal, K.K. (1999). *100 Statistical Test*. Thousand Oaks, California: SAGE Publications Ltd (1999). 215 pages.

Kuang, S. L. (1996). *Geodetic Network Analysis and Optimum Design: Concepts and Applications*. Chelsea, Michigan: Ann Arbor Press, Inc.

Lichti, D. D. (2007). Error Modelling, Calibration and Analysis of an AM-CW Terrestrial Laser Scanner System. *ISPRS Journal of Photogrammetry & Remote Sensing* 61, 2007: 307-324.

Lichti, D. D. (2010). A Review of Geometric Models and Self-Calibration Methods for Terrestrial Laser Scanner. *Bol. Ciênc. Geod., sec. Artigos*, Curitiba, 2010:3-19.

Lichti, D. D. and Chow, J. (2013). Inner Constraints for Planar Features. *Journal of The Photogrammetric Record* 28 (141), 2013: 74-85.

Lichti, D. D., Chow, J. and Lahamy, H. (2011). Parameter De-Correlation and Model-Identification in Hybrid-Style Terrestrial Laser Scanner Self-Calibration. *ISPRS Journal of Photogrammetry and Remote Sensing* 66, 2011:317-326.

Lichti, D.D. and Licht, M. G. (2006). Experiences with Terrestrial Laser Scanner Modelling and Accuracy Assessment. *IAPRS Volume XXXVI*, Part 5, Dresden, 2006:155-160.

Mohd Azwan, A., Halim, S., Zulkepli, M., Albert K. C., Lau C. L., Farid M. A. and Khairulnizam M. I (2013). Improvement in Accuracy for Three-Dimensional Sensor (Faro Photon 120 Scanner). *International Journal of Computer Science Issues*, Volume 10, Issue 1, January 2013:176-182.

Mohd Azwan, A., Halim, S., Zulkepli, M., Albert K. C., Lau C. L., Mohd Farid, M. A. and Khairulnizam, M. I. (2013). Improvement in Accuracy for Three-Dimensional Sensor (Faro Photon 120 Scanner). *International Journal of Computer Science Issues*, Volume 10, Issue 1, January 2013.

Reshetyuk, Y. (2009). *Self-Calibration and Direct Georeferencing in Terrestrial Laser Scanning*. Doctoral Thesis in Infrastructure, Royal Institute of Technology (KTH), Stockholm, Sweden, 2009.

Schneider, D. (2009). Calibration of Riegl LMS-Z420i based on a Multi-Station Adjustment and a Geometric Model with Additional Parameters. *The International Archives of the Photogrammetry, Remote Sensing and Spatial Information Sciences*, 38 (Part 3/W8), 2009: 177-182.

BIOGRAPHICAL NOTES

Mohd Azwan Abbas received the B.Sc. (2004) And M.Sc. (2006) in Geomatic Engineering from Universiti Teknologi Malaysia. He is a Ph.D. student, Department of Geomatic Engineering, Universiti Teknologi Malaysia. His current interests include the calibration and 3D modeling using terrestrial laser scanner.

Halim Setan received M.Sc. (1988) in Geodetic Science from The Ohio State University, Columbus, USA and Ph.D. (1995) in Engineering Surveying from The City University, London, England. He is a Professor, Department of Geomatic Engineering, Universiti Teknologi Malaysia. His current interests include spatial data adjustment, deformation analysis, ground penetration radar and the use of optical and range sensors for 3D reconstruction.

Zulkepli Majid received the M.Sc (1998), B.Sc. (2004) And Ph.D. (2006) in geomatic engineering from Universiti Teknologi Malaysia. He is an Associate Professor, Department of Geomatic Engineering, Universiti Teknologi Malaysia. His current interests include the use of optical and range sensors for 3D reconstruction.

Albert Kon-Fook Chong received the Ph.D. (1986) from University of Washington. He is a Senior Lecturer, Department of Geomatic Engineering, University of Southern Queensland, Australia. His primary research focus is on the use of optical and range imagery for automated 3D object reconstruction.

Derek D. Lichti received the M.Sc. (1996) And Ph.D. (1999) from University of Calgary, Canada. He is a Professor, Department of Geomatic Engineering, University of Calgary, Canada. His primary research focus is on the use of optical and range imagery for automated 3D object reconstruction.

Khairulnizam M. Idris received M.Sc (2003), B.Sc. (2001) And Ph.D. (2011) in geomatic engineering from Universiti Teknologi Malaysia. He is a Senior Lecturer, Department of Geomatic Engineering, Universiti Teknologi Malaysia. His current interests include spatial data adjustment, deformation analysis, Industrial measurement and 3D mapping via unmanned aerial vehicle.

Mohd Farid Mohd Ariff received the M.Sc (2004), B.Sc. (2002) And Ph.D. (2011) in geomatic engineering from Universiti Teknologi Malaysia. He is a Senior Lecturer, Department of Geomatic Engineering, Universiti Teknologi Malaysia. His current interests include photogrammetry approach for 3D modeling and the use of optical and range sensors for high accuracy forensic measurement.

CONTACTS

Mohd Azwan Abbas
Universiti Teknologi MARA, Malaysia
Department of Geomatic Sciences, Universiti Teknologi MARA
Arau, Perlis
MALAYSIA
Email: mohdazwanabbas@gmail.com

Responses for the Reviewers Comments

1st Reviewer

1. There are many problems with the layout of the paper (e.g. Figure 1, Equation 13, Figure 2, an isolated period in the middle of p 9). Equations should be indented for clarity. Units should be given in Table 1. In this table if a0, b0, b1 and c0 refer to Equations 6, 7 and 8 they should be referenced. Why are there quotation marks after b0, b1 and c0.

Answer:

- All equations were indented accordingly.
- Units have been given in Table 1 and equation 6, 7 and 8 were referred as suggested.
- The quotation marks represent the units for b0, b1 and c0, however, all marks have been removed as shown in Table 1.

2. The discussion concerning Figures 4 to 8 on pp 10 to 12 including Table II is not clear. Because of its importance it should be rewritten.

Answer: The discussion has been rewritten as suggested (Section 5/ page 12/ paragraph 4,5 and 6).

3. There are several grammatical errors that could be addressed to improve clarity. For example the sentence: “After the scanning and target measurement processes were completed, the bundle adjustment was performed with precision settings based on the manufacturer’s specification, which were 2mm for distance and 0.009° for both angle measurements.” is long
- Answer:** Manuscript has been sent to professional for proodread.

2nd Reviewer

1. This paper may require proof-reading by a native English speaker. The acronym ‘TLSs’ does not look well and should (and could) be generally replaced by ‘TLS’. Similarly, in the title Terrestrial Laser Scanners should be singular. One reference is quoted but not listed.

Answer:

- Manuscript has been sent to profesional for proodread..
- All acronym TLSs have been changed to TLS as well as the title.
- The reference has been quoted as follow: Gopal, K.K. (1999). *100 Statistical Test*. Thousand Oaks, California: SAGE Publications Ltd (1999). 215 pages.